Evidence for spin mixing in holmium thin film and crystal samples

I. T. M. Usman, K. A. Yates, J. D. Moore, and K. Morrison
The Blackett Laboratory, Physics Department, Imperial College London, London SW7 2AZ, United Kingdom

V. K. Pecharsky and K. A. Gschneidner
Ames Laboratory, U.S. Department of Energy, Iowa State University, Ames, Iowa 50011-3020, USA

T. Verhagen and J. Aarts
Kamerlingh Onnes Laboratory, Leiden Institute of Physics, P.O. Box 9504, 2300 RA Leiden, The Netherlands

V. I. Zverev
Department of Physics, M.V. Lomonosov Moscow State University, Leninskie gory, Moscow, 119992, Russia

J. W. A. Robinson, J. D. S. Witt, and M. G. Blamire
Department of Materials Science and Metallurgy, University of Cambridge, Pembroke Street, Cambridge CB2 3QZ, United Kingdom

L. F. Cohen
The Blackett Laboratory, Physics Department, Imperial College London, London SW7 2AZ, United Kingdom

In a number of recent experiments, holmium has been shown to promote spin-triplet pairing when in proximity to a spin-singlet superconductor. The condition for the support of spin-triplet pairing is that the ferromagnet should have an inhomogeneous magnetic state at the interface with the superconductor. Here we use Andreev reflection spectroscopy to study the properties of single ferromagnet/superconductor interfaces formed of holmium and niobium, as a function of the contact resistance of the junction between them. We find that both single-crystal and c-axis-oriented thin-film holmium show unusual behavior for low junction contact resistance, characteristic of spin-mixing-type properties, which are thought necessary to underpin spin-triplet formation. We also explore whether this signature is observed when the junction is formed of $Ni_{0.19}Pd_{0.81}$ and niobium.

PACS number(s): 74.45.+c, 72.25.Mk, 75.70.−i, 74.50.+r

I. INTRODUCTION

At a superconductor/ferromagnet (S/F) junction conventional spin-singlet Cooper pairs penetrating into the ferromagnet will decay over a length of the order of $\xi_F = \sqrt{\frac{\hbar D_F}{E_{ex}}}$ due to destruction of the Cooper pair coherence as a result of the exchange field of the ferromagnet[1] (where D_F is the diffusion coefficient and E_{ex} is the exchange energy in the ferromagnet[2,3]). In strong ferromagnets E_{ex} is large and ξ_F is of the order of ∼1 nm at low temperature; however, theories have emerged recently suggesting the existence of a exotic proximity effect where spin-triplet pairing is generated at the S/F interface, resulting in a greatly extended decay length, $\xi_T \gg \xi_F$. This exotic proximity effect, named the "long-range spin-triplet proximity effect" (LRSTPE),[4,5] only exists if either some form of inhomogeneous magnetization is present at the S/F interface or if there is a spin-active region (such as spin scattering in a strong spin-orbit coupled medium) between the S and F layers.[4,5] Current thinking suggests that the inhomogeneous magnetic state could either be provided by a magnetic system that offers intrinsic inhomogeneity due to a noncollinear spin arrangement or could be artificially created in a number of ways, including the presence of domain walls (although domain-wall density may prove an issue), or through a thin-film multilayer arrangement using different types of ferromagnets.[6] Either way, spin mixing

must occur close to the interface with the interrogating superconductor.

It has been suggested that holmium (Ho) could provide the necessary magnetic inhomogeneity to induce the LRSTPE due to the intrinsically nonlinear cone structure of its ordered magnetic moments.[7] Indeed, two recent experiments report evidence for triplet pairing promoted by Ho.[8,9] Sosnin *et al.* used Andreev interferometry to measure phase-periodic conductance oscillations in Ho which formed the barrier of a Al/Ho/Al ring structure,[8] while Robinson *et al.* measured the critical current behavior of Nb/Ho/Co/Ho/Nb junctions.[9] Both experiments varied the thickness of the F layers (Ho and Co, respectively) and observed supercurrent signatures with thicknesses much greater than ξ_F.

Evidence for the LRSTPE has been observed also in other systems, including $Pd_{0.88}Ni_{0.12}$ and $Pd_{0.987}Fe_{0.013}$ coupled to Co in $S/F1/N/F2/N/F1/S$-type junctions,[2] Co nanowires with W superconducting leads,[10] and CrO_2, a half-metallic oxide coupled to NbTi or MoGe superconducting leads.[11,12] In these systems the origin of LRSTPE is more likely to be related to artificially created inhomogeneity, either through the difference in spin scattering generated by the choice of thin films in the multilayer stack or though the particular arrangement that a polycrystalline random alignment of grains may present to the superconducting interface. Reviewing these experimental results shows that there is a great deal more to be

learned in this emerging field and, as predicted theoretically, the induced spin-triplet pairing is intimately linked to the properties of the interface. In view of the current status of the field it seems essential to examine the transport across S/F interfaces in more detail so that nature of the spin-singlet to spin-triplet conversion process can be better understood and possibly even controlled.

For any single S/F interface theory tells us that the conductance across the interface plays a pivotal role in determining whether the conventional even-frequency singlet[13] proximity component or the odd-frequency triplet[4] LRSTPE dominates.[14,15] This balance between the singlet and triplet components is due to the competition between the effect of increasing spin mixing (which acts to destroy singlet pairing) and increasing junction transparency (which acts to provide a higher proportion of singlet Cooper pairs from the superconductor). Consequently, for constant, but sufficient, spin-mixing conditions, lower junction transparency (higher interface resistance) should promote the LRSTPE phase while for cleaner junctions (low interface resistance) singlet pairing will dominate. Point-contact Andreev reflection (PCAR) offers a potentially ideal probe as the conductance of the contact (and therefore the S/F interface resistance) can be controlled by varying the pressure on the tip-sample contact. In this paper we examine the properties of single S/F interfaces, primarily those formed between Nb and Ho, and use Andreev spectroscopy to extract details on how the properties of the interface change as the interface transparency is varied. We compare the Nb/Ho results to those obtained from junctions formed between Nb and copper foil and Nb and a $Ni_{0.19}Pd_{0.81}$ thin film.

II. EXPERIMENTAL

Holmium is a rare-earth metal with a complex magnetic phase diagram.[16,17] As the temperature is reduced from room temperature, Ho first undergoes a transition to a spin-spiral antiferromagnetic (AFM) state with a Néel temperature of $T_N \sim 133$ K.[16] In a previous study it was shown using polarized x-ray Bragg diffraction that there were domains of different chirality in the AFM state of a Ho single crystal.[18] Below 19 K (the Curie temperature, T_C) there is a transition to a weak ferromagnetic alignment with a conelike structure where the cone axis lies along the crystallographic c axis in zero applied magnetic field [see the illustration in the inset of Fig. 1(b)].

The Ho single crystal studied here was $(2.44 \times 1.82 \times 0.9)$ mm in size and was grown at the Ames Laboratory using strain annealing.[19] The 300-nm-thick Ho thin film was prepared in a UHV system by dc magnetron sputtering onto a 200-nm-thick Nb buffer on $\sim(5 \times 5)$ mm area heated (~ 873 K) c-plane sapphire. The Ho target was presputtered for 15 min prior to film growth and the system's base pressure was better than 10^{-8} Pa. The films are epitaxial and c-axis oriented as determined by x-ray diffraction. The total Ho thin-film thickness was determined by low-angle x-ray diffraction and by fitting the period of the Kiessig fringes using simulation software. The films were capped with a 10-nm protective layer of gold to prevent surface oxidation. A number of polycrystalline $Ni_{0.19}Pd_{0.81}$ thin films (108 nm) were also prepared for comparative measurements. These films were grown by sputter deposition in a UHV chamber on a Si substrate, as described
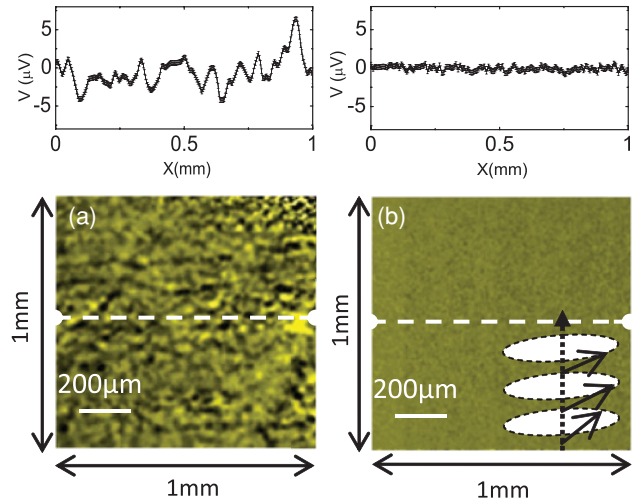

FIG. 1. (Color online) Hall images of (a) single-crystal and (b) thin-film Ho at zero field and 6 K. Black regions represent negative induction and bright regions represent positive induction. Line scans across the center of the images (white dashed lines) are shown in the top panels. Inset to (b) shows a schematic of the cone structure in Ho for $T<19$ K; the dashed arrow corresponds to the direction of the c axis and solid arrows represent the ferromagnetic vectors locked out of plane.

previously.[20] The $Ni_{0.19}Pd_{0.81}$ films have a Curie temperature of 230 K, determined from magnetometry measurements and an easy axis out of the plane. The slightly higher Curie temperature in comparison to the earlier report[20] is probably due to a small change in the surface composition of the target. A copper film prepared by sputtering was used as a benchmark to show how the extracted parameters vary with tip pressure for a nonmagnetic film.

PCAR measurements were taken at 4.2 K using superconducting tips that were mechanically cut from 0.25-mm-diam Nb wire.[21] Spectra were also taken using platinum tips to identify nonsuperconductivity-related components to the "background" conductance spectra.[22] All measurements were performed with the tip aligned parallel to the c axis of the Ho crystal or Ho thin film, which is the ideal crystallographic direction as it lies along the spin cone axis [see the inset of Fig. 1(b)]. The tip-sample distance was controlled by a stepper motor connected to a differential screw such that systematic measurements could be made as a function of contact pressure. In addition to PCAR measurements, the surfaces of the Ho single crystal and thin film were scanned using a Hall probe[23] to identify any variation in the magnetic properties between the crystal and the thin film.

The Andreev spectra were fitted as described previously,[21] using the Blonder-Tinkham-Klapwijk (BTK) equations modified for spin polarization by Mazin *et al.*[24,25] Spectra were fitted for the polarization P, the dimensionless parameter Z, which incorporates the interface scattering, and a smearing parameter ω, which accounts for both thermal and inelastic broadening effects. As any effect of the LRSTPE on the conductance spectra is expected to be subtle, the spectra were fitted using a fixed value for the gap voltage of $\Delta = 1.5$ meV, i.e., the Nb gap value at low temperature.[26] Restricting the fitting routine to a

three-parameter fit ensured that the fitting was robust and that any error introduced by the fitting procedure was systematic across the series. It is usual to define the contact resistance of a junction at zero bias, R_{C0}. However, as the interface properties change drastically with tip pressure, we have extracted the 30-mV resistance at each junction (R_{CB}), and use this value to define the contact resistance.

III. RESULTS

Figure 1 shows the scanning Hall probe images of the out-of-plane magnetic moment in the single crystal oriented in the c axis and in zero applied magnetic field. The noise floor of the 5-μm Hall probe used was ~0.3 μV with a 7.7 mV/T sensitivity. While the crystal shows a considerable moment directed along the c axis [Fig. 1(a)], the signal from the film (which has approximately three orders of magnitude smaller volume) is below the noise floor of the Hall probe sensor [Fig. 1(b)]. We show the results on the film for completeness. The line scans taken across the center of both samples are shown in the top frames in Figs. 1(a) and 1(b). Although it is not possible to determine the chiral sense of the domains with the scanning Hall probe, the size and distribution of the domains indicated in Fig. 1(a) are consistent with (and remarkably similar to) the chiral domain structures in the AFM state observed using circularly polarized x-rays by Lang *et al.*[18]

The evolution of the PCAR spectra with contact resistance (R_{CB}) for the Ho single crystal and Ho thin film are shown in Figs. 2(a) and 2(d), respectively. The data for the $Ni_{0.19}Pd_{0.81}$ film are shown in Fig. 2(f). The high bias dips on the spectra have been associated with the critical current being exceeded in the contact region.[27] In order to fit the data, the spectra for the single crystal were normalized to the conductance spectra obtained using a nonsuperconducting Pt tip, as shown in Fig. 2(b). For the crystal, the background conductance was typically V shaped using either the Pt or Nb tip, and because of the similarity of this feature, we were able to normalize the spectra taken with the Nb tip using the Pt tip spectra as shown in Fig. 2(c). Compared to the crystal, the background spectra obtained on the film were consistently featureless and flat, which meant that the spectra could be normalized directly by the high bias conductance value [Fig. 2(e)]. The fitted spectra generated using the Mazin model are shown in Figs. 2(c) and 2(e) for the crystal and film, respectively, and Fig. 2(g) for the $Ni_{0.19}Pd_{0.81}$ film.

Fitting to the spectra shown in Fig. 2 allows the extraction of the polarization P and (dimensionless) interface parameter Z and the relationship between P and Z for the crystal and film are shown in Figs. 3(a) and 3(b), respectively. The P-Z relationship of a S/F interface always takes a similar form in that high P is associated with low Z and vice versa, and the origin of this dependence has been widely discussed in the literature.[28–32] The "intrinsic" polarization is usually obtained by extrapolating a P-Z plot to low Z—although not usually to $Z = 0$ (Ref. 29) because Z also includes the effect of Fermi velocity mismatch between the S/F materials.[33] The trends we find for the P-Z relationship are not unusual in this respect. However, when we show the explicit relationship of P and Z
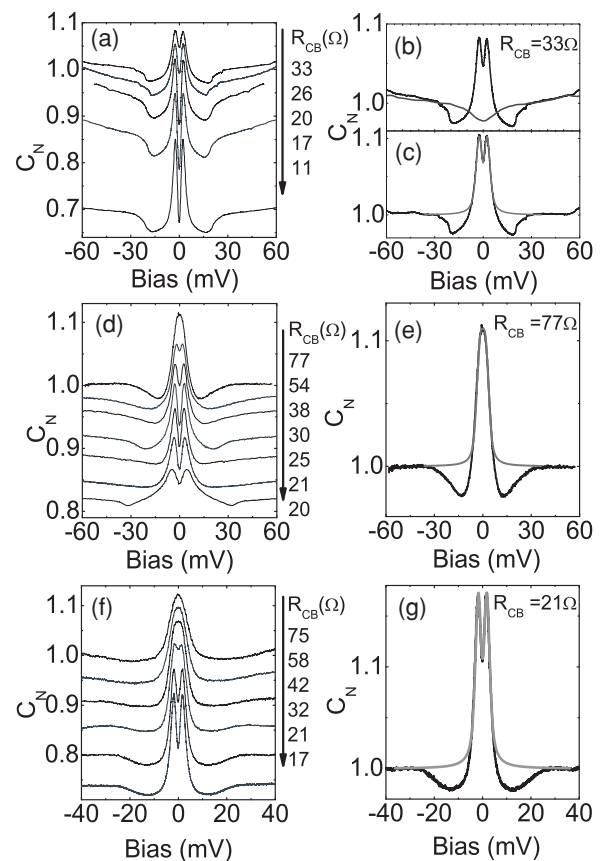

FIG. 2. Point-contact Andreev reflection data at 4.2 K; C_N is the normalized conductance. (a) Normalized conductance spectra as a function of R_{CB} for the Ho crystal. (b) High R_{CB} spectrum taken with a Nb tip (black line) and with a Pt tip (gray line) for the Ho crystal. (c) Same spectrum as (b), but after normalization and fitting (with fitted parameters $\Delta = 1.5$ meV, $\omega = 1.24$ meV, $P = 19.5\%$, $Z = 0.63$). (d) Normalized conductance spectra as a function of R_{CB} for the Ho film. (e) Spectrum taken with a Nb tip shows a flatter background than in the crystal case, so can be fitted using the high bias conductance as shown (fitted parameters $\Delta = 1.5$ meV, $\omega = 1.18$ meV, $P = 35.5\%$, $Z = 0.32$). (f) C_N as a function of R_{CB} for a $Ni_{0.19}Pd_{0.81}$ film. (g) Normalized spectrum and fit from the data set in (f) (with fitted parameters $\Delta = 1.5$ meV, $\omega = 0.72$ meV, $P = 27.5\%$, $Z = 0.41$). The arrows in (a), (d), and (f) indicate decreasing contact resistance. All curves have been offset in the vertical scale for clarity.

with the contact resistance, R_{CB}, of the junction, it becomes clear that the P-Z plot masks a much less obvious relationship.

Figures 4(a) and 4(b) show the behavior of three separate contacts made to the single crystal and Figs. 4(c) and 4(d) show the equivalent for two separate contacts made to the thin film. Both sets of spectra change in an unusual way with increased tip pressure. In both types of samples, as tip pressure is increased (decreasing R_{CB}), Z increases anomalously and sharply, and P shows a corresponding precipitous drop. By direct examination of the spectra shown in Fig. 2, it is clear that the sharpening of spectral features as R_{CB} drops indicates that the effective interface barrier is increasing. This is most clear in Fig. 2(a), the series of spectra taken on the Ho crystal. We are confident that these changes to the Z and P parameters are real (i.e., not an artifact of the fitting process). Furthermore,
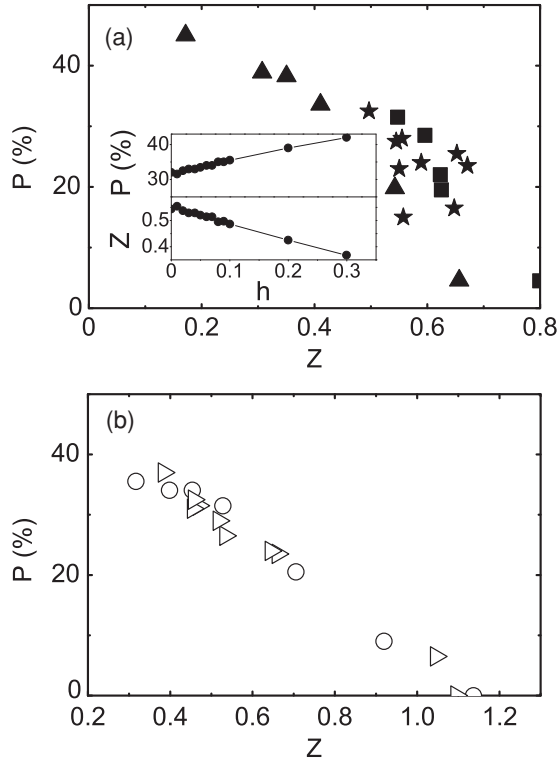
FIG. 3. $P(Z)$ relation on the Ho crystal (a) and Ho thin film (b). Symbols represent different contacts. The inset to (a) is a simulation of the effects of increasing the normalized field $h = H/H_{C2}$ (where H_{C2} is the upper critical field of Nb) using the datum point associated with $R_{CB\,peak}$ shown in Fig. 4(a).

in case of the crystal, the data for $P(R_{CB})$ and $Z(R_{CB})$ show a domelike and a diplike nonmonotonic dependence. We make this more clear in Figs. 4(a) and 4(b) by plotting P,Z as function of $R_{CB}/R_{CB\,peak}$, where $R_{CB\,peak}$ is the value of R_{CB} at the peak in the polarization. For the film, the peak in polarization or dip in Z value is not observed [Fig. 4(c)]. Instead, at higher R_{CB}, the polarization is constant, then starts to decrease with decreasing R_{CB}. The differences between the Ho film and crystal are subtle—what they have in common is that both show the anomalous rise in Z and drop in P at a high tip pressure.

In order to show how anomalous this behavior is, we show the equivalent P and Z behavior when a Nb tip is pressed into a copper foil, or for a Nb tip on a $Ni_{0.19}Pd_{0.81}$ film, plotted in Figs. 4(c) and 4(d). In the case of Cu, Z decreases slightly as R_{CB} is reduced, owing to the increasing transparency of the tip-sample interface[21] (for Cu, $P = 0\%$). In the case of $Ni_{0.19}Pd_{0.81}$, hardly a change in P or Z is found. Note that the difference in behavior of Z in the Ho cannot be explained purely by an increase in the smearing parameter with decreasing contact resistance, as both the Ho crystal and the Cu sample show the same trend of decreased smearing as the contact resistance is reduced.[28]

Before drawing any definitive conclusion, it is also important to try to eliminate any artificial trend in P and Z in the case of the Nb/Ho contact due to the effects of stray magnetic fields on tip properties.[31] In order to examine this in more detail, we have taken the spectrum at the onset to the anomalous rise in Z (and precipitous drop in P) and modeled the effect on this
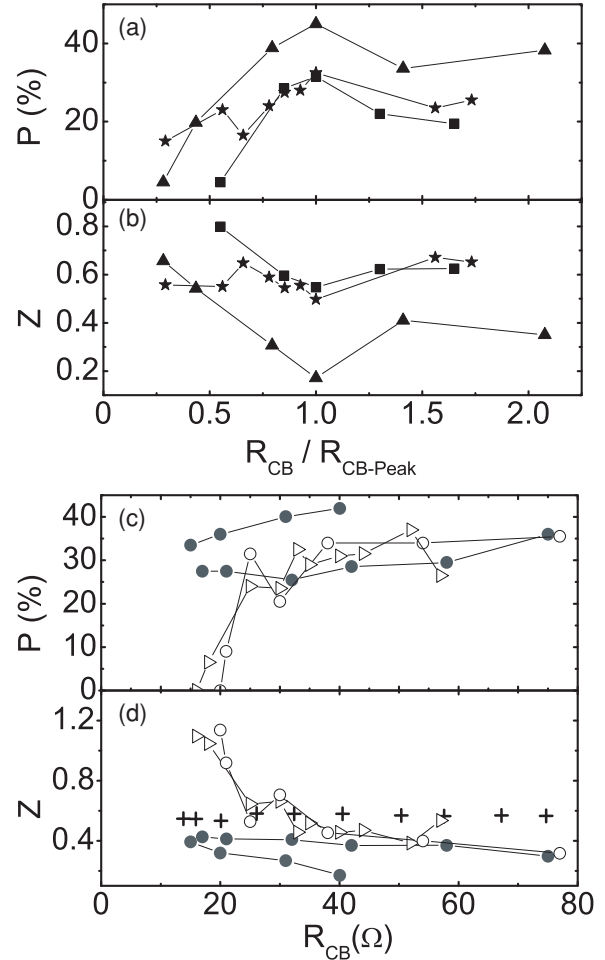

FIG. 4. Dependence of (a) P and (b) Z of the Ho crystal as function of $R_{CB}/R_{CB\,peak}$, where $R_{CB\,peak}$ is the value of R_{CB} at the peak in the polarization with $R_{CB\,peak} = 20$, 39, and 41 Ω for the squares, triangles, and stars in (a) and (b), respectively. The dependence of (c) P and (d) Z on R_{CB} for the spectra taken on the Ho thin film (unfilled symbols), the $Ni_{0.19}Pd_{0.81}$ thin film (filled circles), and copper foil (cross symbols).

spectrum of the presence of an external magnetic field. We do this by using a model we developed previously called "the two-channel model," which we have shown simulates the effect of a magnetic field on the tip properties up to a field of $\sim$80% of the upper critical field H_{C2} of the Nb tip (i.e., $h = H/H_{C2} = 0.8$). The results of this simulation are shown in the inset to Fig. 3(a) up to $h = 0.3$. The plots show that if the effect of increasing tip pressure was simply to experience an increasing magnetic field, P would increase and Z would decrease. This is opposite to the observations that we have made in the main plots of Fig. 4 and therefore we can rule out any possible effects from stray fields. The apparent increase in the Z parameter as the contact resistance drops indeed appears to be a real and anomalous effect. We suggest that it is indicative of a unique form of spin scattering which also results in a reduced P.

IV. DISCUSSION

Theoretical calculations of the expected Andreev conductance spectra in the presence of the LRSTPE[34–37] indicate
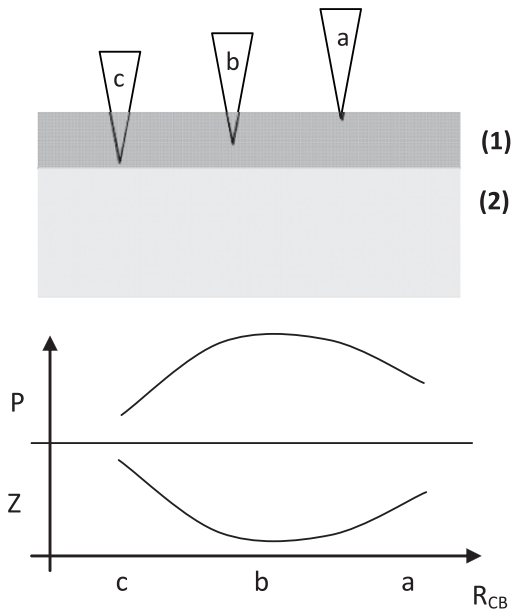
FIG. 5. Schematic illustrating the behavior of P and Z as a function of tip pressure for a system with a surface scattering layer. Layer (1) is a thin surface oxide and layer (2) represents bulk Ho.

that spin mixing at the S/F interface leads to an enhancement of the subgap conductance, either via a direct increase in the conductance [34] or via the formation of Andreev bound states.[36] A number of experimental reports have shown possible signatures of the LRSTPE,[38–40] although it remains to be determined what the "signature" of the LRSTPE is in the Andreev reflection spectra. It is clear, however, from both theoretical and experimental works that if the LRSTPE can be reliably turned "on" and "off," changes should be observed in the parameters used to *fit* the spectra that indicate the subgap conductance, i.e., P and Z. Although we see clear changes in P and Z with R_{CB}, we do not see any evidence of a subgap structure in the spectra (Fig. 2). However, the magnitude of the subgap conductance expected as a result of spin mixing or the LRSTPE may be below the resolution of the spectra shown.[41–43] The changes in P and Z suggest that the scattering mechanism probed by the PCAR at low R_{CB} is an indication of spin mixing that is the precursor to the LRSTPE (i.e., P is reduced as the scattering increases).

The dependence of $P, Z(R_{CB})$ can be understood qualitatively using a simple schematic, as shown in Fig. 5. The behavior of Z at high R_{CB} in the Ho crystal implies the existence of a surface layer, probably an oxide, as proposed for other systems.[44] For the crystal, as the Nb tip first approaches the Ho [Fig. 5(a)], the surface layer acts as a spin-scattering layer, resulting in a low P (and high Z) in the conventional way. As the tip is pushed further into the crystal surface [Fig. 5(b)],

the Andreev reflection probes the spin alignment of the Ho with a Z parameter that is indicative of a clean interface and the observed P is maximal. Finally, as the tip goes through this surface layer completely [Fig. 5(c)], the spin mixing of the Ho becomes dominant (Z increases) and so P is once again reduced. In the case of the film, the thin Au capping layer prevents the oxide from forming, and so as the tip first approaches the capped film surface, the intrinsic P of the Ho is preserved through the thin metallic capping layer and P is approximately constant with R_{CB}. Once the tip punctures the capping layer, the intrinsic spin mixing of the Ho results in the same high Z value and low P behavior, as observed in the Ho crystal. The results indicate that, at low R_C in both the crystal and the film, spin mixing occurs. Note that, in PCAR, R_{CB} can decrease either due to a cleaner interface or due to an increase in the physical size of the contact.[30,44] This may explain why the effects observed here vary in magnitude between different contacts [for example, the square and star datasets in Fig. 4(a)].

Figures 4(c) and 4(d) also shows our first results on a 108-nm-thick $Ni_{0.19}Pd_{0.81}$ film. The spectra and fit to a spectrum are shown in Figs. 2(f) and 2(g). Interestingly, although reports that thin films (<4 nm) of $Pd_{0.88}Ni_{0.12}$ promote triplet behavior,[2] here we see no significant anomalous upturn in Z as compared with Ho. However, this result is consistent with the view that, whereas in Ho the spin-triplet state is promoted by the intrinsic inhomogeneity of the spin state of the material, in the multilayer stack, the inhomogeneous magnetization has been created artificially and that a $Ni_{0.19}Pd_{0.81}$ film would not necessarily be expected to support proximity-induced spin-triplet behavior in isolation. Our inference concerning NiPd agrees with the recent publication from the Birge group.[45]

In conclusion, we have shown an anomalous dependence of the polarization P and the interface scattering parameter Z on contact resistance R_{CB} in the magnetically inhomogeneous system Ho, using point-contact Andreev reflection spectroscopy. Similarities in the PCAR spectra taken on both single-crystal and thin-film Ho suggest a common scattering mechanism. This scattering results in reduced polarization and strongly suggests increased spin mixing, a fundamental precursor to the LRSTPE effect. We do not see this effect when we perform the same experiments using copper foil or $Ni_{0.19}Pd_{0.81}$ thin films.

[1] E. A. Demler, G. B. Arnold, and M. R. Beasley, Phys. Rev. B **55**, 15174 (1997).

[2] T. S. Khaire, M. A. Khasawneh, W. P. Pratt, and N. O. Birge, Phys. Rev. Lett. **104**, 137002 (2010).

[3] F. S. Bergeret, A. F. Volkov, and K. B. Efetov, Phys. Rev. Lett. **86**, 3140 (2001).

[4] F. S. Bergeret, A. F. Volkov, and K. B. Efetov, Rev. Mod. Phys. **77**, 1321 (2005).

[5] M. Eschrig and T. Lofwander, Nat. Phys. **4**, 138 (2008).

[6] J. W. A. Robinson, G. B. Halasz, A. I. Buzdin, and M. G. Blamire, Phys. Rev. Lett. **104**, 207001 (2010).

[7] G. B. Halasz, J. W. A. Robinson, J. F. Annett, and M. G. Blamire, Phys. Rev. B **79**, 224505 (2009).

[8] I. Sosnin, H. Cho, V. T. Petrashov, and A. F. Volkov, Phys. Rev. Lett. **96**, 157002 (2006).

[9] J. W. A. Robinson, J. D. S. Witt, and M. G. Blamire, Science **329**, 59 (2010).

[10] J. Wang *et al.*, Nat. Phys. **6**, 389 (2010).

[11] R. S. Keizer, S. T. B. Goennenwein, T. M. Klapwijk, G. X. Miao, G. Xiao, and A. Gupta, Nature (London) **439**, 825 (2006).

[12] M. S. Anwar, F. Czeschka, M. Hesselberth, M. Porcu, and J. Aarts, Phys. Rev. B **82**, 100501(R) (2010).

[13] A. I. Buzdin, Rev. Mod. Phys. **77**, 935 (2005).

[14] J. Linder, A. Sudbo, T. Yokoyama, R. Grein, and M. Eschrig, Phys. Rev. B **81**, 214504 (2010).

[15] J. Linder, T. Yokoyama, A. Sudbo, and M. Eschrig, Phys. Rev. Lett. **102**, 107008 (2009).

[16] W. C. Koehler, J. W. Cable, M. K. Wilkinson, and E. O. Wollan, Phys. Rev. **151**, 414 (1966).

[17] W. C. Koehler, J. W. Cable, H. R. Child, M. K. Wilkinson, and E. O. Wollan, Phys. Rev. **158**, 450 (1967).

[18] J. C. Lang, D. R. Lee, D. Haskel, and G. Srajer, J. Appl. Phys. **95**, 6537 (2004).

[19] D. L. Strandburg, S. Legvold, and F. H. Spedding, Phys. Rev. **127**, 2046 (1962).

[20] C. Cirillo, A. Rusanov, C. Bell, and J. Aarts, Phys. Rev. B **75**, 174510 (2007).

[21] Y. Bugoslavsky, Y. Miyoshi, S. K. Clowes, W. R. Branford, M. Lake, I. Brown, A. D. Caplin, and L. F. Cohen, Phys. Rev. B **71**, 104523 (2005).

[22] A. I. Akimenko and I. K. Yanson, Pis'ma Zh. Eksp. Teor. Fiz. **31**, 209 (1980) [JETP Lett. **31**, 191 (1980)].

[23] G. K. Perkins, Y. V. Bugoslavsky, X. Qi, J. L. MacManus-Driscoll, and A. D. Caplin, IEEE Trans. Appl. Supercond. **11**, 3186 (2001).

[24] I. I. Mazin, A. A. Golubov, and B. Nadgorny, J. Appl. Phys. **89**, 7576 (2001).

[25] G. E. Blonder, M. Tinkham, and T. M. Klapwijk, Phys. Rev. B **25**, 4515 (1982).

[26] C. Kittel and P. McEuen, *Introduction to Solid State Physics* (Wiley, New York, 2005).

[27] G. Sheet, S. Mukhopadhyay, and P. Raychaudhuri, Phys. Rev. B **69**, 134507 (2004).

[28] C. H. Kant, O. Kurnosikov, A. T. Filip, P. LeClair, H. J. M. Swagten, and W. J. M. de Jonge, Phys. Rev. B **66**, 212403 (2002).

[29] G. T. Woods, R. J. Soulen, I. I. Mazin, B. Nadgorny, M. S. Osofsky, J. Sanders, H. Srikanth, W. F. Egelhoff, and R. Datla, Phys. Rev. B **70**, 054416 (2004).

[30] G. J. Strijkers, Y. Ji, F. Y. Yang, C. L. Chien, and J. M. Byers, Phys. Rev. B **63**, 104510 (2001).

[31] Y. Miyoshi, Y. Bugoslavsky, and L. F. Cohen, Phys. Rev. B **72**, 012502 (2005).

[32] Y. Ji, G. J. Strijkers, F. Y. Yang, C. L. Chien, J. M. Byers, A. Anguelouch, G. Xiao, and A. Gupta, Phys. Rev. Lett. **86**, 5585 (2001).

[33] G. E. Blonder and M. Tinkham, Phys. Rev. B **27**, 112 (1983).

[34] Y. Q. Ji, Z. P. Niu, C. D. Feng, and D. Y. Xing, Chin. Phys. Lett. **25**, 691 (2008).

[35] A. Kadigrobov, R. I. Shekhter, and M. Jonson, Low Temp. Phys. **27**, 760 (2001).

[36] R. Grein, T. Lofwander, G. Metalidis, and M. Eschrig, Phys. Rev. B **81**, 094508 (2010).

[37] C. Di Feng, Z. M. Zheng, Y. Q. Ji, Z. P. Niu, and D. Y. Xing, J. Appl Phys. **103**, 023921 (2008).

[38] V. N. Krivoruchko and V. Y. Tarenkov, Phys. Rev. B **78**, 054522 (2008).

[39] K. A. Yates, W. R. Branford, F. Magnus, Y. Miyoshi, B. Morris, L. F. Cohen, P. M. Sousa, O. Conde, and A. J. Silvestre, Appl. Phys. Lett. **91**, 172504 (2007).

[40] B. Almog, S. Hacohen-Gourgy, A. Tsukernik, and G. Deutscher, Phys. Rev. B **80**, 220512(R) (2009).

[41] E. H. Zhao, T. Lofwander, and J. A. Sauls, Phys. Rev. B **70**, 134510 (2004).

[42] J. Brauer, F. Hubler, M. Smetanin, D. Beckmann, and H. von Lohneysen, Phys. Rev. B **81**, 024515 (2010).

[43] F. Hubler, M. J. Wolf, D. Beckmann, and H. v. Lohneysen, e-print arXiv:1012.3867v1 (2010).

[44] K. A. Yates, A. J. Behan, J. R. Neal, D. S. Score, H. J. Blythe, G. A. Gehring, S. M. Heald, W. R. Branford, and L. F. Cohen, Phys. Rev. B **80**, 245207 (2009).

[45] M. A. Khasawneh, T. S. Khaire, C. Klose, W. P. Pratt, and N. O. Birge, Supercond. Sci. Technol. **24**, 024005 (2011).